

# The Geometric Origin of Time's Arrow: Loschmidt Resolved

Ira Wolfson

Department of Electronics and Electrical Engineering, Braude College of Engineering,  
Karmiel 2161002, Israel  
wolfsoni@braude.ac.il

December 5, 2025

## Abstract

We resolve Loschmidt's paradox—the 150-year-old contradiction between time-reversible microscopic dynamics and irreversible macroscopic evolution. The resolution requires both quantum mechanics and classical chaos; neither alone suffices. Quantum uncertainty without chaos produces slow, polynomial spreading—not fundamentally irreversible. Classical chaos without quantum uncertainty produces computational intractability—trajectories diverge exponentially, yet the system remains on one trajectory, reversible in principle with sufficient precision. Only together do they produce geometric impossibility: chaos exponentially amplifies irreducible  $\hbar$ -scale uncertainty until stable manifolds contract below quantum resolution, rendering time-reversed trajectories physically inaccessible despite being mathematically valid and equiprobable. Information is never destroyed—it becomes geometrically inaccessible. The Kolmogorov-Sinai entropy rate is identical in both time directions, preserving microscopic symmetry while explaining macroscopic irreversibility. Three decades of Loschmidt echo experiments confirm perturbation-independent decay consistent with geometric inaccessibility. The framework unifies thermodynamic, quantum, and information-theoretic arrows of time.

## 1 Introduction

Time flows forward. Eggs scramble but never unscramble. Gases mix but never unmix. Heat flows from hot to cold, never reversing. Yet the microscopic laws governing atoms and molecules—Newton's mechanics, Maxwell's electromagnetism, Schrödinger's equation—are perfectly time-reversible. Every allowed trajectory has an equally valid time-reversed twin.

In 1876, Loschmidt crystallized this into a paradox[1]. Consider nitrogen gas at room temperature. Measure positions and momenta at  $t = 0$ , evolve for five seconds, then reverse all momenta. Since Hamilton's equations are time-symmetric, the system should retrace its trajectory exactly. Entropy should decrease, violating the second law. Thus either the laws of dynamical evolution break, or the second law does. Yet both are experimentally inviolate. This is the paradox.

We resolve it completely. The resolution requires recognizing that **irreversibility emerges from the intersection of quantum mechanics and classical chaos—neither alone suffices**. Quantum uncertainty produces slow spreading; classical chaos produces computational intractability. Only together do they produce geometric impossibility: chaos exponentially amplifies the irreducible  $\hbar$ -scale uncertainty until stable manifolds contract below quantum resolution. Time-reversed trajectories exist mathematically but cannot be accessed physically. This is not a practical limitation—it is geometric necessity.

## 2 Why Existing Approaches Fail

Before presenting our resolution, we must understand why 150 years of attempts have failed.

**“Molecular chaos” (Boltzmann’s Stosszahlansatz)[2].** Assume velocities are uncorrelated before collisions but not after. But this explicitly breaks time-reversal symmetry—we have inserted the arrow of time by hand. Loschmidt’s entire objection was that such asymmetric assumptions are unjustified.

**“Coarse-graining” (Penrose, Gibbs)[3].** We don’t track exact microstates, only macroscopic bins. As phase space stretches and folds, the distribution spreads across more bins. But this is circular: *why* can we not track exact microstates? What determines the coarse-graining scale? Unless we identify a *physical boundary* that prevents arbitrary precision, we have explained nothing.

**“It’s about information” (Jaynes)[4, 5].** Entropy measures observer ignorance. But if entropy is purely subjective, why does it universally increase? Different observers with different information should see different entropy evolution. They don’t.

**“Special initial conditions” (Past Hypothesis)[6, 7].** The universe started in a low-entropy state at the Big Bang; that is why entropy increases. But this fails to address Loschmidt’s scenario. Start with *any* state—low or high entropy—evolve it forward, then reverse all momenta. Either the system returns to its initial conditions (violating the second law), or entropy continues increasing despite the reversal. One of the two must give. Cosmology is irrelevant.

**“It’s statistically unlikely.”** Entropy decrease is possible but improbable. But Loschmidt’s theorem proves that  $P(\Gamma) = P(\bar{\Gamma})$ —the time-reversed trajectory has *exactly equal probability*. There is no statistical asymmetry to invoke.

**None of these responses resolves the paradox.** They miss the point (cosmology), invoke circular reasoning (coarse-graining without physical basis), contradict Loschmidt’s theorem (statistical arguments), or beg the question (assume time asymmetry). The paradox has stood for 150 years because something fundamental was missing.

## 3 What Entropy Actually Measures

The system *is* in one specific microstate—one configuration. This is ontological reality. But we typically know only macroscopic constraints: energy  $E$ , volume  $V$ , particle number  $N$ . Limiting entropy to microstate-macrostate relations is shortsighted—entropy fundamentally measures our uncertainty about which configuration the system occupies. This interpretation naturally falls out of, for example, the Sackur-Tetrode formula for gases, spin-lattice combinatorics, and Planck’s photon statistics:

$$S = k_B \ln \Omega \tag{1}$$

where  $\Omega$  counts configurations consistent with constraints. The system is in *one* configuration. We don’t know which.

For spins and photons, configurations are already discrete—no coarse-graining needed. For continuous phase space (gases, liquids), we must specify a minimum cell size to make configurations countable. That cell is  $(2\pi\hbar)^3$  per particle—not an arbitrary choice but a physical necessity. Heisenberg uncertainty forbids distinguishing points closer than  $\hbar$  in phase space:

$$\Delta x \cdot \Delta p \geq \frac{\hbar}{2} \tag{2}$$

Below this scale, “different configurations” has no physical meaning. Zurek recognized this in his analysis of sub-Planck structures[8]: phase space can develop structure finer than  $\hbar$ , but this structure is

physically inaccessible—it cannot be measured, prepared, or exploited. This is where Jaynes meets Penrose: entropy is epistemic (about knowledge), but the boundaries of knowledge are ontic (physically determined by  $\hbar$ ).

However, quantum coarse-graining alone does not resolve Loschmidt. A system could remain near its initial state indefinitely if dynamics were non-chaotic. What has been missing is the recognition that chaos is equally essential: it exponentially amplifies  $\hbar$ -scale uncertainty to macroscopic scales on physically relevant timescales. Neither quantum mechanics nor chaos alone produces irreversibility—only their intersection does.

## 4 The Single-Particle Arrow of Time

The arrow of time does not require many particles, collisions, or chaos. It appears for a single free particle.

At  $t = 0$ , prepare a particle in a minimum-uncertainty state: one Planck cell,  $\Delta x \cdot \Delta p = 2\pi\hbar$ , entropy  $S = 0$ . Now let it evolve freely. The wavepacket spreads:

$$\Delta x(t) = \sqrt{\Delta x_0^2 + \left(\frac{2\pi\hbar t}{m\Delta x_0}\right)^2} \quad (3)$$

No collisions. No chaos. No ensemble. Just Schrödinger evolution. The particle remains in *one* microstate, but we no longer know which Planck cell it occupies. Entropy grows because we started with finite precision and uncertainty spreads with time.

This is the most fundamental arrow of time. Thermodynamics, statistical mechanics, the second law—all compound this same mechanism across  $10^{23}$  particles, with chaos accelerating what quantum uncertainty initiates.

Integrable systems—the harmonic oscillator being the paradigm—represent the reversible limit, the Carnot cycle of quantum mechanics. Coherent states maintain minimum uncertainty indefinitely; entropy remains constant. But no real system is perfectly integrable. Anharmonicity is ubiquitous, and with it, chaos.

## 5 Neither Alone Suffices

Here is the key insight that has been missing for 150 years:

**Quantum uncertainty without chaos** produces the wavepacket spreading above—slow, polynomial growth. Information about the microstate remains accessible. This is not fundamental irreversibility.

**Classical chaos without quantum uncertainty** produces exponential trajectory divergence. Two nearby initial conditions separate as  $\delta(t) \sim \delta_0 e^{\lambda t}$ , where  $\lambda$  is the Lyapunov exponent. Prediction becomes computationally intractable. But—and this is crucial—the system is still on *one* trajectory. With sufficient precision in specifying initial conditions, reversal remains possible in principle. Chaos creates practical difficulty, not fundamental impossibility.

**Both together** produce geometric impossibility. Start with initial preparation uncertainty  $\delta_0$ —bounded below by  $\hbar$  but typically much larger (thermal fluctuations, experimental resolution). Chaos amplifies uncertainty along unstable manifolds:  $\delta_{\text{unstable}}(t) \sim \delta_0 \cdot e^{\lambda t}$ . Simultaneously, stable manifolds contract:

$\delta_{\text{stable}}(t) \sim \delta_0 \cdot e^{-\lambda t}$ . After time  $t \sim \lambda^{-1} \ln(\delta_0/\hbar)$ , stable manifolds have contracted below  $\hbar$ —below the scale where quantum mechanics permits distinctions.

To reverse the trajectory, we must specify initial conditions within the stable manifolds. But these have contracted below  $\hbar$ . The required precision is not merely difficult—it is forbidden by Heisenberg uncertainty. The information needed for reversal exists (Liouville’s theorem guarantees phase space volume is conserved), but it is encoded in sub-quantum structure that cannot be accessed, measured, or exploited.

**This is the resolution.** Time-reversed trajectories are mathematically valid and equiprobable—Loschmidt was right. But they are geometrically inaccessible. Information is not destroyed; it becomes inaccessible. This inaccessibility *is* the arrow of time.

## 6 Mathematical Derivation

We now derive the critical time  $t_c$  beyond which reversal becomes geometrically impossible. (Full details in Supplementary Information.)

Consider a Hamiltonian system with phase-space coordinates  $\Gamma \in \mathbb{R}^{2N}$ . The flow  $\phi_t : \Gamma_0 \mapsto \Gamma(t)$  is symplectic, hence volume-preserving (Liouville). For a reference trajectory  $\Gamma^*(t)$ , nearby deviations evolve as  $\delta\Gamma(t) = \mathbf{M}(t) \cdot \delta\Gamma(0)$ , where the stability matrix satisfies  $\mathbf{M}^T \mathbf{J} \mathbf{M} = \mathbf{J}$ . This symplectic condition forces eigenvalues to pair as  $(\mu, 1/\mu)$ , implying Lyapunov exponents pair as  $(\lambda, -\lambda)$ .

The tangent space decomposes into unstable ( $E^u$ ,  $\lambda_i > 0$ ) and stable ( $E^s$ ,  $\lambda_i < 0$ ) subspaces. Under forward evolution:

$$\sigma_u(t) \sim \delta_0 \cdot e^{+\lambda t} \quad (\text{unstable: expands}) \quad (4)$$

$$\sigma_s(t) \sim \delta_0 \cdot e^{-\lambda t} \quad (\text{stable: contracts}) \quad (5)$$

Volume is conserved; shape is radically altered. The initial uncertainty sphere becomes an exponentially elongated, exponentially thin filament. Repeated stretching and folding creates fractal structure at all scales—but quantum mechanics truncates this structure at  $\hbar$ , below which the fractal is physically meaningless.

The Kolmogorov-Sinai entropy  $h_{KS} = \sum_{\lambda_i > 0} \lambda_i$  measures the information loss rate—the rate at which microscopic information becomes inaccessible to observation.<sup>1</sup> By Lyapunov pairing,  $h_{KS}^{\text{forward}} = h_{KS}^{\text{backward}}$ : information becomes inaccessible at identical rates in both time directions. The arrow of time is not in the dynamics.

Quantum mechanics provides the resolution scale. States differing by less than  $\ell_{\hbar} \equiv \sqrt{\hbar}$  cannot be prepared, measured, or distinguished—they are not distinct physical entities. The threshold crossing occurs when:

$$\sigma_s(t_c) = \delta_0 e^{-\lambda t_c} = \ell_{\hbar} \quad (6)$$

giving the critical time:

$$t_c = \frac{1}{\lambda} \ln \left( \frac{\delta_0}{\ell_{\hbar}} \right) \quad (7)$$

For gases at STP:  $\delta_0/\ell_{\hbar} \sim 10^6$ ,  $\lambda \sim 10^{10} \text{ s}^{-1}$ , yielding  $t_c \sim 1 \text{ ns}$ .

<sup>1</sup>In dynamical systems theory,  $h_{KS}$  is conventionally called the “information production rate” because coarse-grained entropy increases. Here we use “loss rate” to emphasize that information is not destroyed but rendered inaccessible, which is the physically relevant quantity for irreversibility.

Before  $t_c$ : reversal is exponentially hard. After  $t_c$ : reversal requires sub-quantum precision—not difficult but meaningless. The Loschmidt fidelity undergoes sigmoid decay around  $t_c$ :

$$F(t) \approx \frac{1}{2} \operatorname{erfc} \left( \frac{t - t_c}{\sqrt{2}\sigma_t} \right) \quad (8)$$

This sigmoid shape—a threshold crossing, not exponential leakage—is the experimental discriminant. Loschmidt echo experiments confirm perturbation-independent sigmoid decay, consistent with the geometric mechanism[12, 13].

Neither chaos nor quantum mechanics alone produces irreversibility. Chaos without  $\hbar$ : reversal is hard but not impossible. Quantum resolution without chaos: no contraction toward threshold. Only together do they yield geometric inaccessibility.

## 7 Spaghettification of Phase Space

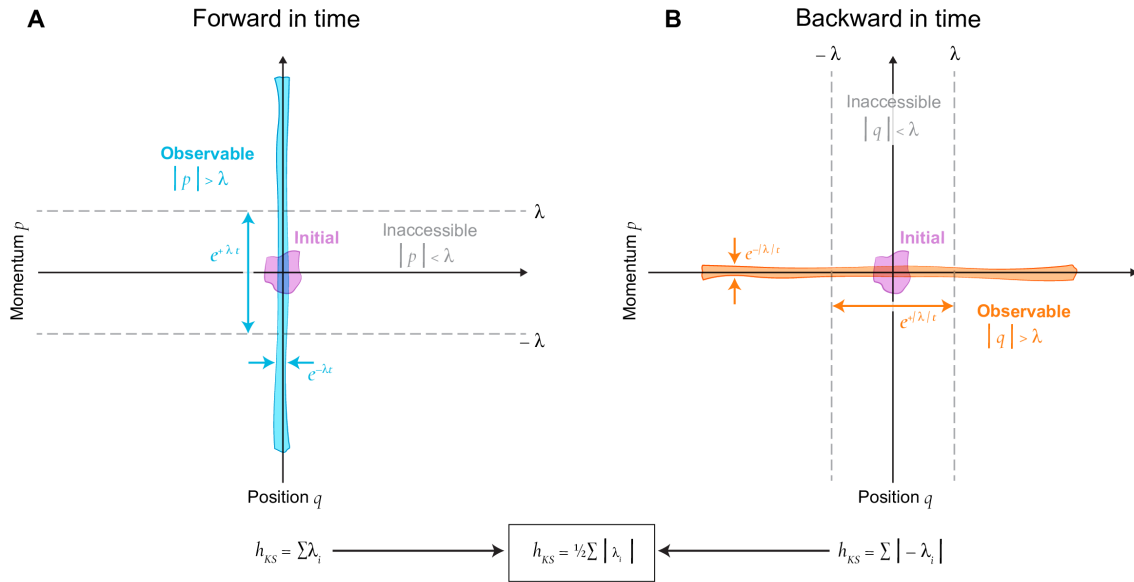


Figure 1: **Symmetric information loss in both time directions.** **A:** Forward evolution stretches phase space along unstable manifolds while contracting along stable manifolds below quantum resolution  $\hbar$ . **B:** Backward evolution reverses which manifold expands. Both directions yield identical Kolmogorov-Sinai entropy  $h_{KS} = \frac{1}{2} \sum |\lambda_i|$ .

For Hamiltonian systems, Lyapunov exponents come in positive-negative pairs (symplectic structure):

$$\{\lambda_1, -\lambda_1, \lambda_2, -\lambda_2, \dots\}, \quad \sum_i \lambda_i = 0 \quad (9)$$

This pairing is why Liouville’s theorem holds: what stretches in one direction compresses in another, preserving total volume. But entropy increases because the number of distinguishable Planck cells grows. Distinct initial microstates get “spaghettified” into the same coarse-grained cell, their differences along compressed dimensions converging into sub- $\hbar$  structure. Phase space transforms into the higher-dimensional analogue of a space-filling curve.

The Kolmogorov-Sinai entropy quantifies the information loss rate[9, 10]:

$$h_{KS} = \sum_{\lambda_i > 0} \lambda_i \quad (10)$$

Under time reversal,  $\lambda_i \rightarrow -\lambda_i$ , but  $|\lambda_i|$  is invariant:

$$h_{KS}^{\text{forward}} = h_{KS}^{\text{backward}} \Rightarrow h_{KS} = \frac{1}{2} \sum_i |\lambda_i| \quad (11)$$

This reformulation makes it explicit that information becomes inaccessible at identical rates in both time directions. The dynamics are perfectly symmetric. The asymmetry emerges from which manifolds remain above quantum resolution—and those are always the expanding ones, by definition.

“Forward in time” simply means “the direction along which we observe expansion of accessible phase space.” This is universal because stable manifolds *always* contract below  $\hbar$ , regardless of which direction we call forward.

## 8 Quantitative Impossibility

For nitrogen gas at room temperature, the maximum Lyapunov exponent is:

$$\lambda_{\max} = \frac{\ln(\lambda_{\text{mfp}}/d)}{\tau_{\text{coll}}} \approx 3 \times 10^{10} \text{ s}^{-1} \quad (12)$$

To reverse after time  $t$  and return to the initial state, momentum precision must satisfy:

$$\delta p_{\text{required}} < \sqrt{mk_B T} \cdot e^{-h_{KS} \cdot t} \quad (13)$$

The quantum limit is  $\delta p_{\text{quantum}} = \sqrt{mk_B T}$ . Therefore:

$$\frac{\delta p_{\text{required}}}{\delta p_{\text{quantum}}} \sim e^{-h_{KS} \cdot t} \quad (14)$$

Even under maximally conservative assumptions—shortest timescale where kinetic theory applies ( $t = 1$  ns), single-mode chaos ( $h_{KS} = \lambda_{\max}$ ):

$$\frac{\delta p_{\text{required}}}{\delta p_{\text{quantum}}} \sim e^{-30} \approx 10^{-13}$$

(15)

Reversal after one nanosecond requires precision thirteen orders of magnitude beyond quantum limits. This is not a practical difficulty—it is **geometric impossibility**.

At macroscopic times ( $t = 1$  second):

$$\frac{\delta p_{\text{required}}}{\delta p_{\text{quantum}}} \sim e^{-3 \times 10^{10}} \approx 10^{-10^{10}} \quad (16)$$

The required precision is  $10^{10}$  billion orders of magnitude beyond quantum limits.

But there is a deeper problem. Even if we could somehow achieve perfect reversal—knowing both initial and final microstates exactly—we would still face combinatorial impossibility. A macrostate contains

$\Omega \approx e^{S/k_B}$  distinct microstates. After evolution and reversal back to the initial macrostate,  $\Omega$  microstates are again consistent with what we observe. Which one are we in? The many-to-one mapping between microstates and macrostates creates  $\Omega^2$  possible pairings. Even perfect macroscopic reversal does not imply microscopic trajectory reversal—we cannot verify the system retraced its path rather than taking one of the  $e^{S/k_B}$  other trajectories connecting the same endpoints.

## 9 Experimental Confirmation: Loschmidt Echoes

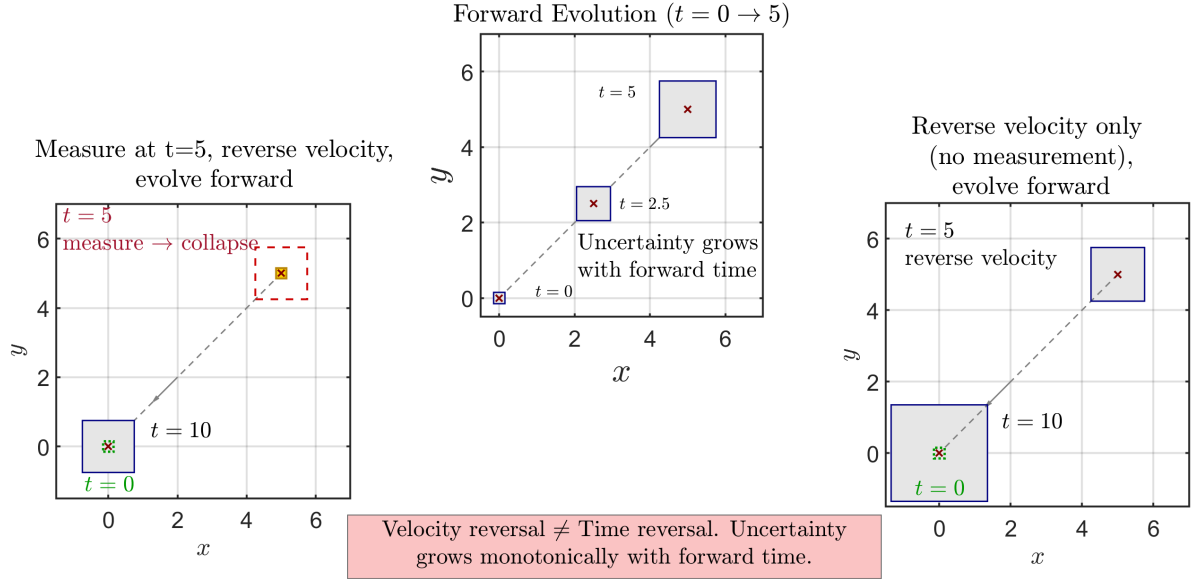


Figure 2: **Velocity reversal does not constitute time reversal.** Center: Forward evolution; uncertainty grows. Left: Measure, reverse velocity, evolve—centroid returns but uncertainty regrows. Right: Reverse velocity without measurement—uncertainty continues growing. Entropy grows monotonically regardless of velocity direction.

The geometric mechanism predicts specific experimental signatures, tested over three decades of Loschmidt echo experiments[11, 12, 13, 14].

The protocol: prepare an initial state, evolve forward under Hamiltonian  $H$ , then attempt reversal by evolving under  $-H$  (achieved via NMR pulse sequences). The echo amplitude  $M(t)$  measures return fidelity.

If irreversibility were merely practical—imperfect pulses, environmental noise—decay should depend on perturbation strength. Instead, Pastawski and collaborators discovered that decay persists at a rate determined by intrinsic system properties, independent of perturbation strength[13, 14].

The functional form is sigmoid, not exponential:

$$M(t) \propto \left(1 + e^{-\sigma^2(t-t_c)^2}\right)^{-1} \quad (17)$$

This threshold behavior is the signature of geometric inaccessibility. Fidelity remains high while stable manifolds stay above quantum resolution. At critical time  $t_c$ , they cross the threshold—and fidelity collapses. The width of the sigmoid represents what we might call the “Lazarus window”—the brief interval during which information hovers at the quantum threshold, not yet irretrievably lost. Once this window closes, information has fallen into sub-Planckian perdition. The perturbation-independent, sigmoid decay confirms that irreversibility emerges from geometry, not technical limitations.

## Numerical Simulation

To test the geometric mechanism directly, we simulated Loschmidt echo in the Bunimovich stadium billiard—a paradigmatic chaotic system with well-characterized Lyapunov exponent (Fig. 3). An ensemble of  $M$  particles evolves forward for time  $T$  under exact Hamiltonian dynamics, undergoes velocity reversal with a small perturbation  $\varepsilon = 0.01$  to the boundary radius, then evolves backward for time  $T$ . The fidelity  $F(T, \delta)$  measures the fraction of particles returning within coarse-graining scale  $\delta$  of their initial phase-space position.

The results confirm three key predictions of the geometric framework. First, fidelity decays as a sigmoid rather than exponentially (Fig. 3f), the signature of threshold crossing rather than continuous leakage. Second, the critical time scales as  $t_c = \lambda^{-1} \ln(\delta/\varepsilon)$  with fitted slope  $1/\lambda = 3.49$  (Fig. 3c), consistent with the predicted logarithmic dependence on resolution. Third,  $t_c$  is independent of ensemble size  $M$  (Fig. 3b,e), with mean variation below 2.5% across two orders of magnitude in  $M$ . This  $M$ -independence is the smoking gun: irreversibility emerges from individual trajectory geometry, not statistical effects. The contours in panel (b) are horizontal—the transition time depends only on resolution  $\delta$ , not on how many particles we simulate. Details of the simulation algorithm and parameter choices are provided in Supplementary Information. The stadium billiard represents the simplest possible chaotic system—single-particle chaos from boundary geometry alone. Many-body systems with particle-particle collisions exhibit higher Lyapunov exponents and faster threshold crossing, compounding rather than weakening the geometric mechanism.

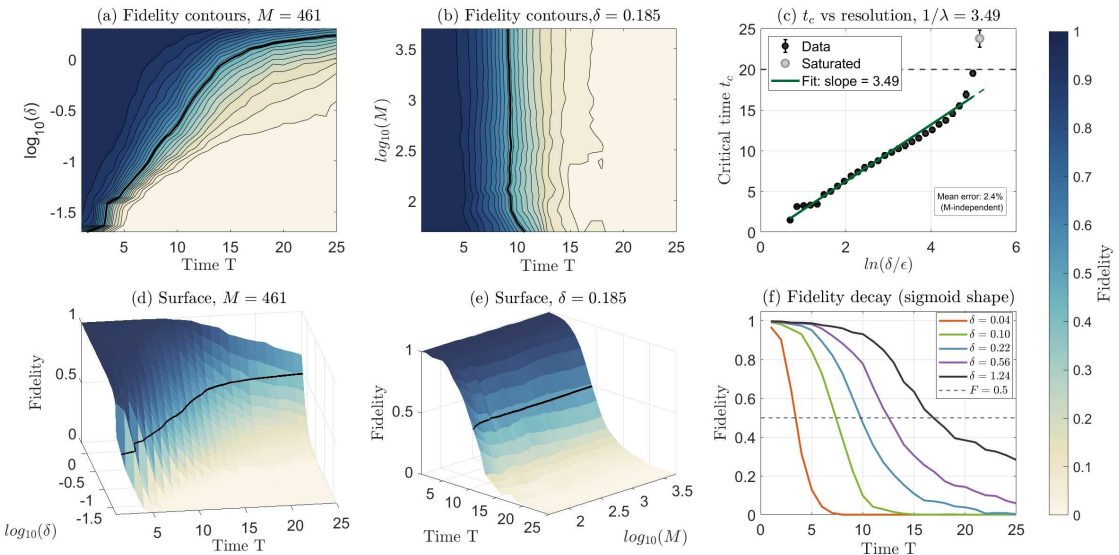


**Figure 3: Numerical confirmation of geometric irreversibility in stadium billiard.** (a) Fidelity contours versus time  $T$  and coarse-graining  $\delta$  at fixed ensemble size  $M = 461$ . The diagonal ridge marks the transition from reversible ( $F \approx 1$ ) to irreversible ( $F \approx 0$ ). (b) Fidelity contours versus  $T$  and  $M$  at fixed  $\delta = 0.185$ ; horizontal contours confirm  $M$ -independence. (c) Critical time  $t_c$  versus  $\ln(\delta/\varepsilon)$  shows the predicted linear scaling with slope  $1/\lambda = 3.49$ . Error bars (mean variation 2.4%) confirm  $t_c$  is determined by geometry, not statistics. Gray points exceed simulation window (saturation artifact). (d,e) Three-dimensional surfaces corresponding to panels (a,b). (f) Fidelity decay curves for different  $\delta$  values exhibit characteristic sigmoid shape, not exponential tails. Perturbation  $\varepsilon = 0.01$ .

## 10 Falsifiable Predictions

The framework generates quantitative predictions distinct from competing interpretations:

**Quantum simulators.** Loschmidt echoes in trapped-ion or superconducting qubit systems should exhibit sigmoid decay—not exponential. The critical time  $t_c$  depends on interaction structure and coupling strength. Exponential decay would falsify the geometric mechanism. Current platforms ( $N = 50\text{--}100$  qubits) have sufficient control for decisive tests.

**OTOC saturation.** Out-of-time-order correlators saturate when stable manifolds contract below quantum resolution. The predicted scrambling time  $t_* \sim \lambda_L^{-1} \ln(S/\ln d)$  is testable in quantum dot systems via charge fluctuation measurements.

**Sigmoid vs exponential.** The geometric mechanism predicts threshold behavior (sigmoid), while decoherence models typically predict exponential decay. This functional form is experimentally distinguishable and provides a clean test.

**Relativistic thermodynamics.** The Lorentz invariance of  $\hbar$  and phase-space volume implies entropy is frame-invariant:  $S' = S$ . Combined with thermodynamic identities, this yields temperature transformation  $T' = T/\gamma$ —the Einstein-Planck result[15, 16], contradicting Ott’s  $T' = \gamma T$ [17]. S-stars orbiting Sgr A\* at  $v \sim 0.03c$  offer a natural laboratory: their photospheric spectra encode temperature information that could distinguish these predictions. We are actively developing this test, with detailed predictions for GRAVITY and forthcoming ELT observations to appear separately.

## 11 Conclusion: The 150-Year Paradox Dissolves

Loschmidt’s paradox dissolves when we recognize what has been missing: irreversibility requires both quantum mechanics and classical chaos. Neither alone suffices.

Neither alone breaks time’s symmetry. Together, they shatter it. Chaos exponentially amplifies irreducible  $\hbar$ -scale uncertainty until stable manifolds contract below quantum resolution—phase space drawn into a higher-dimensional space-filling curve. Liouville’s theorem holds. The information is lost to us.

Loschmidt was right: time-reversed trajectories are equally probable. But equiprobability does not guarantee accessibility. Reversal requires sub- $\hbar$  precision—geometric impossibility. Information is never destroyed; it becomes geometrically inaccessible. This inaccessibility *is* the arrow of time.

The Kolmogorov-Sinai entropy rate is identical forward and backward:  $h_{KS}^{\text{forward}} = h_{KS}^{\text{backward}}$ . Microscopic time-reversal symmetry is preserved. The asymmetry is purely epistemic—which manifolds remain above quantum resolution—and those are always the expanding ones.

Three decades of Loschmidt echo experiments confirm perturbation-independent sigmoid decay. Quantitative calculations show nanosecond reversal requires precision thirteen orders of magnitude beyond quantum limits.

Boltzmann’s *Stosszahlansatz* is unnecessary. Coarse-graining is not ad hoc— $\hbar$  is the coarse-graining, and it is mandated by physics, not convention. The Past Hypothesis is not required—entropy increases regardless of initial conditions because information becomes inaccessible at rate  $h_{KS}$  in both time directions.

The second law is not about dynamics being irreversible. It is about information accessibility being geometrically bounded. Time-reversed trajectories exist mathematically but are geometrically inaccessible.

Entropy increases not by statistical accident, not by cosmological initial conditions, but by geometric necessity.

A speculative discussion of whether the same geometric mechanism might extend to Planck-scale dynamics—potentially connecting to the Bekenstein-Hawking entropy—is provided in Supplementary Note 10. This extension remains conjectural and is not required for the resolution presented here.

## Methods

### Lyapunov exponent estimation

For hard-sphere gases,  $\lambda_{\max} \sim \tau_{\text{coll}}^{-1} \ln(\lambda_{\text{mfp}}/d)$ . For nitrogen at 300 K: molecular diameter  $d = 3.7 \times 10^{-10}$  m, mean free path  $\lambda_{\text{mfp}} \approx 8.6 \times 10^{-8}$  m, collision time  $\tau_{\text{coll}} \approx 1.8 \times 10^{-10}$  s.

### Loschmidt echo analysis

Experimental data from Sánchez et al.[14] show sigmoid decay with perturbation-independent rate scaling with intrinsic Hamiltonian properties.

## References

- [1] Loschmidt, J. Über den Zustand des Wärmegleichgewichtes eines Systems von Körpern mit Rücksicht auf die Schwerkraft. *Sitzungsber. Kais. Akad. Wiss. Wien, Math. Naturwiss. Classe* **73**, 128–142 (1876).
- [2] Boltzmann, L. Weitere Studien über das Wärmegleichgewicht unter Gasmolekülen. *Sitzungsber. Kais. Akad. Wiss. Wien, Math. Naturwiss. Classe* **66**, 275–370 (1872).
- [3] Penrose, O. *Foundations of Statistical Mechanics* (Pergamon, Oxford, 1970).
- [4] Jaynes, E. T. Information theory and statistical mechanics. *Phys. Rev.* **106**, 620–630 (1957).
- [5] Jaynes, E. T. Information theory and statistical mechanics II. *Phys. Rev.* **108**, 171–190 (1957).
- [6] Albert, D. Z. *Time and Chance* (Harvard University Press, 2000).
- [7] Carroll, S. *From Eternity to Here: The Quest for the Ultimate Theory of Time* (Dutton, 2010).
- [8] Zurek, W. H. Sub-Planck structure in phase space and its relevance for quantum decoherence. *Nature* **412**, 712–717 (2001).
- [9] Kolmogorov, A. N. Entropy per unit time as a metric invariant of automorphisms. *Dokl. Akad. Nauk SSSR* **124**, 754–755 (1959).
- [10] Sinai, Ya. G. On the notion of entropy of a dynamical system. *Dokl. Akad. Nauk SSSR* **124**, 768–771 (1959).
- [11] Levstein, P. R., Usaj, G. & Pastawski, H. M. Attenuation of polarization echoes in NMR. *J. Chem. Phys.* **108**, 2718–2724 (1998).
- [12] Pastawski, H. M. *et al.* A NMR answer to the Boltzmann-Loschmidt controversy? *Physica A* **283**, 166–170 (2000).

- [13] Jalabert, R. A. & Pastawski, H. M. Environment-independent decoherence rate in classically chaotic systems. *Phys. Rev. Lett.* **86**, 2490–2493 (2001).
- [14] Sánchez, C. M. *et al.* Perturbation independent decay of the Loschmidt echo. *Phys. Rev. Lett.* **124**, 030601 (2020).
- [15] Einstein, A. Über das Relativitätsprinzip und die aus demselben gezogenen Folgerungen. *Jahrb. Radioakt. Elektron.* **4**, 411–462 (1907).
- [16] Planck, M. Zur Dynamik bewegter Systeme. *Ann. Phys.* **331**, 1–34 (1908).
- [17] Ott, H. Lorentz-Transformation der Wärme und der Temperatur. *Z. Phys.* **175**, 70–104 (1963).

# Supplementary Information: The Geometric Origin of Time's Arrow: Loschmidt Resolved

Ira Wolfson

Department of Electronics and Electrical Engineering, Braude College of Engineering,  
Karmiel 2161002, Israel  
wolfseni@braude.ac.il

December 5, 2025

## Contents

|           |  |          |
|-----------|--|----------|
| <b>1</b>  | <b>Overview</b>  | <b>3</b> |
| <b>2</b>  | <b>Hamiltonian Dynamics and Symplectic Structure</b>         | <b>3</b> |
| <b>3</b>  | <b>The Stability Matrix and Lyapunov Spectrum</b>            | <b>3</b> |
| <b>4</b>  | <b>Kolmogorov-Sinai Entropy</b>                              | <b>4</b> |
| <b>5</b>  | <b>Stable and Unstable Manifolds</b>                         | <b>5</b> |
| <b>6</b>  | <b>The Quantum Resolution Threshold</b>                      | <b>6</b> |
| <b>7</b>  | <b>The Loschmidt Protocol</b>                                | <b>6</b> |
| <b>8</b>  | <b>Fidelity Decay and Experimental Signatures</b>            | <b>7</b> |
| <b>9</b>  | <b>Summary</b>   | <b>7</b> |
| <b>10</b> | <b>Numerical Simulation: Stadium Billiard Loschmidt Echo</b> | <b>8</b> |
| 10.1      | System and Protocol  | 8        |
| 10.2      | Algorithm: Collision Table Method                            | 8        |
| 10.3      | Parameters   | 9        |
| 10.4      | Results  | 9        |
| 10.5      | Saturation Artifact  | 10       |
| 10.6      | Code Availability  | 10       |

|  |           |
|--|-----------|
| <b>11 Speculative Extension: Planck-Scale Horizons (Non-Essential)</b> | <b>10</b> |
| 11.1 Motivation . . . . .  | 10        |
| 11.2 The Bekenstein-Hawking Puzzle . . . . .                           | 10        |
| 11.3 A Possible Geometric Interpretation . . . . .                     | 11        |
| 11.4 Significant Caveats . . . . .                                     | 11        |
| 11.5 Why Include This Speculation? . . . . .                           | 12        |

## 1 Overview

This Supplementary Information provides a complete derivation of the geometric criterion for irreversibility. The central result is the critical time

$$t_c = \frac{1}{\lambda} \ln \left( \frac{\delta_0}{\ell_h} \right) \quad (1)$$

beyond which time reversal requires sub-quantum precision and is therefore physically meaningless. The derivation proceeds through the mathematical machinery of Hamiltonian dynamics, establishing the symplectic structure, Lyapunov spectrum, and stable/unstable manifold geometry before deriving the threshold condition and its experimental signatures.

## 2 Hamiltonian Dynamics and Symplectic Structure

Consider a Hamiltonian system with  $N$  degrees of freedom. We denote by  $\Gamma(\tau) \in \mathbb{R}^{2N}$  a point in phase space and by  $\gamma = \{\Gamma(\tau)\}$  the trajectory passing through it. By the Picard-Lindelöf theorem, each point determines a unique trajectory.

The Hamiltonian flow  $\phi_t : \Gamma_0 \mapsto \Gamma(t)$  is generated by Hamilton's equations:

$$\dot{\Gamma} = J \cdot \nabla_{\Gamma} H, \quad J = \begin{pmatrix} 0 & I \\ -I & 0 \end{pmatrix} \quad (2)$$

where  $J$  is the symplectic matrix. The flow preserves the symplectic 2-form  $\omega = \sum_i dq_i \wedge dp_i$ , which implies Liouville's theorem: phase-space volume is conserved, and fine-grained Gibbs entropy satisfies  $dS/dt = 0$ .

Symplectic evolution includes hyperbolic rotations—transformations that stretch phase space in some directions while compressing in others, preserving total volume. A squeeze of the form  $\text{diag}(e^\lambda, e^{-\lambda})$  is symplectic: it preserves area ( $e^\lambda \cdot e^{-\lambda} = 1$ ) while radically altering shape. This is the classical analog of a Lorentz boost, which is a hyperbolic rotation in spacetime.

The quantum resolution scale  $\hbar$  does not participate in this symplectic flow. While the distribution stretches and compresses,  $\hbar$  remains fixed. Threshold crossings at  $\delta = \hbar$  are therefore physical invariants, not coordinate artifacts.

If  $\gamma$  solves Hamilton's equations, so does its time-reverse  $T\gamma$  under the map  $(q_i, p_i, t) \mapsto (q_i, -p_i, -t)$ . This is Loschmidt's starting point.

We note that Hamiltonian trajectories play the role of geodesics in symplectic geometry, just as free-particle paths are geodesics in Riemannian geometry. The statement  $d\rho/dt = 0$  along trajectories is the symplectic analog of parallel transport along geodesics.

## 3 The Stability Matrix and Lyapunov Spectrum

For a reference trajectory  $\Gamma^*(t)$ , the evolution of nearby deviations  $\delta\Gamma(t) = \Gamma(t) - \Gamma^*(t)$  is governed by the linearized equation:

$$\frac{d}{dt} \delta\Gamma = \mathbf{L}(t) \cdot \delta\Gamma, \quad \mathbf{L}(t) = J \cdot H''(\Gamma^*(t)) \quad (3)$$

where  $H''$  is the Hessian of the Hamiltonian evaluated along the reference trajectory. The solution takes the form  $\delta\Gamma(t) = \mathbf{M}(t) \cdot \delta\Gamma(0)$ , where the stability matrix  $\mathbf{M}(t)$  satisfies:

$$\frac{d\mathbf{M}}{dt} = \mathbf{L}(t) \cdot \mathbf{M}, \quad \mathbf{M}(0) = \mathbf{I} \quad (4)$$

The stability matrix inherits symplectic structure from the flow. To see this, define  $\mathbf{A}(t) = \mathbf{M}^T \mathbf{J} \mathbf{M}$  and differentiate:

$$\frac{d\mathbf{A}}{dt} = \dot{\mathbf{M}}^T \mathbf{J} \mathbf{M} + \mathbf{M}^T \mathbf{J} \dot{\mathbf{M}} = \mathbf{M}^T \mathbf{L}^T \mathbf{J} \mathbf{M} + \mathbf{M}^T \mathbf{J} \mathbf{L} \mathbf{M} \quad (5)$$

Using  $\mathbf{L} = JH''$  and the properties  $J^T = -J$ ,  $J^2 = -\mathbf{I}$ :

$$\frac{d\mathbf{A}}{dt} = \mathbf{M}^T (H'' J^T J + J J H'') \mathbf{M} = \mathbf{M}^T (-H'' + H'') \mathbf{M} = 0 \quad (6)$$

Since  $\mathbf{A}(0) = J$ , we have  $\mathbf{M}^T \mathbf{J} \mathbf{M} = J$  for all  $t$ . Taking determinants yields  $\det(\mathbf{M})^2 = 1$ , and by continuity from  $\mathbf{M}(0) = \mathbf{I}$ , we conclude  $\det(\mathbf{M}) = +1$ . This is Liouville's theorem in matrix form.

The symplectic condition constrains the eigenvalue structure. If  $\mu$  is an eigenvalue of  $\mathbf{M}$ , so is  $1/\mu$  (and for complex eigenvalues, also  $\mu^*$  and  $1/\mu^*$ ). The Lyapunov exponents, defined as the asymptotic growth rates

$$\lambda_i = \lim_{t \rightarrow \infty} \frac{1}{t} \ln \sigma_i(t) \quad (7)$$

where  $\sigma_i(t)$  are the singular values of  $\mathbf{M}(t)$ , therefore come in pairs  $(\lambda, -\lambda)$ . The Oseledets multiplicative ergodic theorem guarantees these limits exist for almost all trajectories in ergodic systems.

The Lyapunov spectrum thus takes the form  $\{\lambda_1, -\lambda_1, \lambda_2, -\lambda_2, \dots, \lambda_N, -\lambda_N\}$  with  $\sum_i \lambda_i = 0$ . This pairing is Liouville's theorem made directional: expansion in unstable directions exactly compensates contraction in stable directions.

Under time reversal  $\mathbf{M}(-t) = \mathbf{M}(t)^{-1}$ , so expanding directions become contracting and vice versa.

## 4 Kolmogorov-Sinai Entropy

The Kolmogorov-Sinai entropy  $h_{KS}$  quantifies the rate at which a dynamical system produces information—equivalently, the rate at which predictive power decays. It is defined as the supremum over all partitions  $\mathcal{P}$  of phase space:

$$h_{KS} = \sup_{\mathcal{P}} \lim_{n \rightarrow \infty} \frac{1}{n} H(\mathcal{P}^{(n)}) \quad (8)$$

where  $H(\mathcal{P}^{(n)})$  is the Shannon entropy of the partition refined over  $n$  time steps.

The supremum removes dependence on arbitrary coarse-graining choices. It is achieved by generating partitions—those whose symbolic dynamics uniquely encodes trajectories. For uniformly hyperbolic systems, Markov partitions constructed from stable and unstable manifolds are generating; their boundaries align with the invariant directions, ensuring that distinct trajectories produce distinct symbol sequences.

For general ergodic systems, Krieger's theorem guarantees existence of finite generating partitions when  $h_{KS} < \infty$ . However, for physical systems this abstraction is unnecessary. Since quantum mechanics forbids distinctions finer than  $\hbar$ , cells of size  $\hbar$  constitute a natural generating partition: no finer distinctions are physically realizable. The KS entropy is therefore well-defined for any physical chaotic system, with

$$h_{KS} = \sum_{\lambda_i > 0} \lambda_i \quad (9)$$

by the Pesin identity.

The time-reversal symmetry of  $h_{KS}$  follows immediately from Lyapunov pairing. Under  $t \rightarrow -t$ , exponents flip sign:  $\lambda_i \rightarrow -\lambda_i$ . The set of positive exponents becomes the set of (magnitudes of) negative exponents, but by pairing these sets are identical:

$$h_{KS}^{\text{forward}} = \sum_{\lambda_i > 0} \lambda_i = \sum_{\lambda_i > 0} |\lambda_i| = h_{KS}^{\text{backward}} \quad (10)$$

Information becomes inaccessible at identical rates in both time directions. The arrow of time cannot reside in  $h_{KS}$ .

## 5 Stable and Unstable Manifolds

The Lyapunov spectrum induces a decomposition of the tangent space at each point  $\Gamma$ :

$$T_\Gamma = E^u \oplus E^s \oplus E^c \quad (11)$$

where  $E^u$  is the unstable subspace (spanned by directions with  $\lambda_i > 0$ ),  $E^s$  is the stable subspace ( $\lambda_i < 0$ ), and  $E^c$  is the center subspace ( $\lambda_i = 0$ ). By Lyapunov pairing,  $\dim(E^u) = \dim(E^s)$ .

These local subspaces extend to global invariant manifolds. The unstable manifold  $W^u(\Gamma)$  consists of all points approaching  $\Gamma$  as  $t \rightarrow -\infty$ ; the stable manifold  $W^s(\Gamma)$  consists of points approaching  $\Gamma$  as  $t \rightarrow +\infty$ . Under forward evolution,  $W^u$  stretches as  $e^{+\lambda t}$  while  $W^s$  contracts as  $e^{-\lambda t}$ .

Volume conservation forces the characteristic stretching-and-folding of chaotic dynamics. An initial uncertainty region elongates along  $W^u$  and thins along  $W^s$ ; since it cannot escape a bounded region, the elongated filament must fold back on itself. After  $n$  Lyapunov times, a region has filament width  $\sim \delta_0 e^{-n}$ , layer count  $\sim e^n$ , and fractal dimension given by the Kaplan-Yorke formula:

$$D_{KY} = k + \frac{\sum_{i=1}^k \lambda_i}{|\lambda_{k+1}|} \quad (12)$$

where  $k$  is the largest integer with  $\sum_{i=1}^k \lambda_i \geq 0$ .

Classically, this fractal structure continues to arbitrarily fine scales. Quantum mechanics truncates it at scale  $\hbar$ . The fractal persists mathematically below  $\hbar$ , but this sub-Planckian structure is physically meaningless—present in the formalism, absent from reality.

This provides the dynamical mechanism for Zurek’s observation that sub-Planck phase space structure, while mathematically present, is physically inaccessible. The mechanism is Lyapunov contraction along stable manifolds; the timescale is  $t_c = \lambda^{-1} \ln(\delta_0/\hbar)$ .

Under time reversal,  $W^u$  and  $W^s$  exchange roles. The dynamics remains symmetric. The asymmetry lies in access: we observe expansion along  $W^u$ , but reversing requires preparing states on the contracted  $W^s$ . For  $t > t_c$ , this demands sub- $\hbar$  precision—geometrically forbidden.

The quantum-mechanical manifestation is scrambling. Out-of-time-order correlators  $C(t) = \langle [W(t), V(0)]^2 \rangle$  measure how local operators spread into non-local correlations. When  $C(t)$  saturates, information about  $V(0)$  is no longer locally accessible. Unitarity guarantees the information survives, encoded in correlations spanning the system, but it is operationally inaccessible. Stable manifold contraction below  $\hbar$  and OTOC saturation are the same threshold in different languages.

## 6 The Quantum Resolution Threshold

Represent initial uncertainty by a distribution  $\rho_0(\Gamma)$  over phase space with characteristic width  $\delta_0$ . Heisenberg uncertainty imposes the lower bound  $\delta_0 \geq \ell_\hbar \equiv \sqrt{\hbar}$ . This is not a measurement limitation but an existence bound: sub- $\hbar$  distinctions do not correspond to distinct physical states.

For thermal systems, the initial uncertainty is set by the de Broglie wavelength  $\delta_0 \sim \lambda_{dB} = \hbar/\sqrt{mk_B T}$ . For gases at standard conditions,  $\delta_0/\ell_\hbar \sim 10^6$ .

Under Hamiltonian evolution, a Gaussian distribution with covariance  $\Sigma_0$  evolves to  $\Sigma(t) = \mathbf{M}(t) \cdot \Sigma_0 \cdot \mathbf{M}(t)^T$ . For isotropic initial uncertainty  $\delta_0$ , the widths along stable and unstable directions evolve as:

$$\sigma_u(t) \sim \delta_0 \cdot e^{+\lambda t} \quad (13)$$

$$\sigma_s(t) \sim \delta_0 \cdot e^{-\lambda t} \quad (14)$$

The initial sphere becomes an exponentially elongated, exponentially thin ellipsoid. Volume is conserved; shape is radically altered. Information is not created or destroyed but redistributed: spreading along  $W^u$  becomes macroscopically observable while contraction along  $W^s$  pushes information below  $\hbar$ .

Classical mechanics permits the stable manifold to contract indefinitely—reversal is exponentially difficult but never impossible in principle. Quantum mechanics changes this fundamentally. The threshold crossing occurs when:

$$\sigma_s(t_c) = \delta_0 e^{-\lambda t_c} = \ell_\hbar \quad (15)$$

Solving for the critical time:

$$t_c = \frac{1}{\lambda} \ln \left( \frac{\delta_0}{\ell_\hbar} \right) \quad (16)$$

For gases at STP with  $\delta_0/\ell_\hbar \sim 10^6$  and  $\lambda \sim 10^{10} \text{ s}^{-1}$ , this yields  $t_c \sim 1 \text{ ns}$ .

Before  $t_c$ , reversal is exponentially hard. After  $t_c$ , reversal requires sub-quantum precision—not difficult but meaningless, like specifying electron position to  $10^{-50} \text{ m}$ . The question has no physical answer.

The Lorentz invariance of  $\hbar$  ensures this threshold is frame-independent. Irreversibility is objective, not observer-dependent.

## 7 The Loschmidt Protocol

The Loschmidt protocol consists of forward evolution for time  $t$ , momentum reversal ( $p_i \rightarrow -p_i$ ), and forward evolution again. Time-reversal symmetry guarantees return to the initial state if reversal is exact.

At the reversal moment, the system state lies on a filament of width  $\sigma_s(t) = \delta_0 e^{-\lambda t}$  along the stable manifold. Correct reversal requires specifying the state to this precision. But any physical preparation introduces uncertainty at least  $\ell_\hbar$ .

For  $t > t_c$ , the required precision falls below  $\ell_\hbar$ . The state we prepare is consistent with approximately  $e^{\lambda(t-t_c)}$  distinct trajectories, each diverging exponentially during the return phase. After time  $t$ , we miss the origin by a factor of order  $\delta_0/\ell_\hbar \sim 10^6$  or worse.

A concrete example illustrates the scale of this impossibility. For nitrogen at STP, reversal at  $t = 1 \text{ ns}$  requires precision  $\delta_0 e^{-\lambda t} \sim 10^{-24} \text{ m}$ . The available precision is  $\ell_\hbar \sim 10^{-17} \text{ m}$ —seven orders of magnitude short.

The dynamics remains exactly time-symmetric. The reversed trajectory exists as a valid solution of Hamilton's equations with equal probability to the forward trajectory. What fails is physical access: we cannot prepare, measure, or verify states at sub- $\hbar$  precision. The arrow of time emerges from symmetric dynamics encountering a fixed resolution scale.

## 8 Fidelity Decay and Experimental Signatures

The Loschmidt fidelity  $F(t) = |\langle \psi_0 | \psi_{2t}^{\text{reversed}} \rangle|^2$  quantifies return after attempted reversal. For  $t < t_c$ , stable manifolds remain above quantum resolution, reversal largely succeeds, and  $F \approx 1$ . For  $t > t_c$ , stable manifolds have contracted below  $\ell_\hbar$ , reversal fails, and  $F \approx 0$ .

The transition between these regimes is sharp because it reflects a threshold crossing, not a continuous decay process. For a system with a single Lyapunov exponent, the transition would be a step function at  $t_c$ . Real systems have a spectrum of exponents  $\{\lambda_i\}$ , each direction crossing threshold at its own critical time  $t_c^{(i)} = \lambda_i^{-1} \ln(\delta_0/\ell_\hbar)$ .

The fidelity factorizes over directions:  $F(t) = \prod_i f_i(t)$ , where each factor transitions from 1 to 0 around its respective  $t_c^{(i)}$ . For many degrees of freedom with a distribution of exponents, the central limit theorem applies. Near the mean critical time  $\bar{t}_c$ :

$$F(t) \approx \frac{1}{2} \text{erfc} \left( \frac{t - \bar{t}_c}{\sqrt{2}\sigma_t} \right) \quad (17)$$

where  $\sigma_t$  is the standard deviation of critical times across directions. This is the characteristic sigmoid shape: plateau near 1 for  $t \ll \bar{t}_c$ , rapid transition around  $\bar{t}_c$ , plateau near 0 for  $t \gg \bar{t}_c$ .

The sigmoid functional form distinguishes the geometric mechanism from decoherence models. Decoherence typically predicts exponential decay  $F(t) \sim e^{-\Gamma t}$  with rate  $\Gamma$  proportional to perturbation strength. The geometric mechanism predicts sigmoid decay with rate set by intrinsic Lyapunov exponents, independent of perturbation strength above a threshold.

Three decades of Loschmidt echo experiments confirm these signatures. Pastawski, Jalabert, and collaborators observed perturbation-independent decay rates determined by intrinsic Hamiltonian properties, sigmoid-like transitions rather than pure exponentials, and saturation at late times rather than continued decay. These observations match the geometric mechanism and would falsify pure decoherence interpretations.

## 9 Summary

Hamiltonian dynamics is exactly time-symmetric and volume-preserving, yet macroscopic irreversibility is universally observed. The resolution lies in the intersection of two facts: chaotic dynamics compresses stable manifolds exponentially, and quantum mechanics truncates physical distinguishability at scale  $\hbar$ .

The logical structure of the argument proceeds as follows. Symplectic structure forces Lyapunov exponents to pair as  $(\lambda, -\lambda)$ , ensuring the Kolmogorov-Sinai entropy—the information loss rate—is identical in both time directions. Stable manifolds contract as  $e^{-\lambda t}$ , creating fractal structure at all scales. Quantum resolution truncates this structure at  $\ell_\hbar = \sqrt{\hbar}$ , establishing a critical time  $t_c = \lambda^{-1} \ln(\delta_0/\ell_\hbar)$ . Beyond  $t_c$ , reversed trajectories exist mathematically but require sub-quantum precision to access—they are geometrically inaccessible.

Neither chaos nor quantum mechanics alone produces irreversibility. Chaos without  $\hbar$  makes reversal exponentially difficult but never impossible in principle; one could always specify initial conditions more

precisely. Quantum mechanics without chaos provides a resolution scale but no mechanism to approach it; uncertainty would remain constant. Only their intersection yields geometric inaccessibility.

This framework resolves Loschmidt's paradox: reversed trajectories are not absent but inaccessible. It resolves Boltzmann's coarse-graining problem:  $\hbar$  provides the cell size, mandated by physics rather than convention. It obviates the Past Hypothesis: irreversibility emerges dynamically from chaos meeting quantum resolution, regardless of cosmological initial conditions.

The experimental prediction is sigmoid fidelity decay—a threshold crossing rather than exponential leakage—with perturbation-independent rate set by Lyapunov exponents. Loschmidt echo experiments confirm this signature.

The microscopic laws remain exactly time-symmetric. The arrow of time emerges from symmetric dynamics encountering a fixed, frame-independent resolution scale.

## 10 Numerical Simulation: Stadium Billiard Loschmidt Echo

### 10.1 System and Protocol

The Bunimovich stadium billiard consists of two semicircular caps of radius  $R$  connected by straight walls of length  $2a$ . We use natural units  $R = a = 1$ , particle speed  $|v| = 1$ . The stadium is a paradigmatic chaotic system: almost all trajectories are ergodic with positive Lyapunov exponent  $\lambda \approx 0.3\text{--}1$  depending on geometry.

The Loschmidt echo protocol proceeds as follows:

1. Initialize  $M$  particles with random positions uniformly distributed inside the stadium and random velocity directions (all with  $|v| = 1$ ).
2. Evolve forward for time  $T$  under exact collision dynamics with boundary radius  $R$ .
3. Reverse all velocities:  $\mathbf{v} \rightarrow -\mathbf{v}$ .
4. Evolve backward for time  $T$  under perturbed dynamics with boundary radius  $R' = R(1 + \varepsilon)$ .
5. Reverse velocities again and measure phase-space distance from initial state.

The fidelity is defined as

$$F(T, \delta) = \frac{1}{M} \sum_{i=1}^M \Theta(\delta - d_i(T)) \quad (18)$$

where  $d_i(T) = \sqrt{|\mathbf{r}_i^{\text{final}} - \mathbf{r}_i^{\text{initial}}|^2 + |\mathbf{v}_i^{\text{final}} - \mathbf{v}_i^{\text{initial}}|^2}$  is the Euclidean distance in 4-dimensional phase space  $(x, y, v_x, v_y)$ , and  $\Theta$  is the Heaviside step function.

### 10.2 Algorithm: Collision Table Method

We employ an event-driven algorithm with exact collision detection, avoiding numerical integration errors entirely. The method maintains a collision table storing the predicted time to each wall for each particle.

**Initialization:** For each particle  $n$  and each wall  $w \in \{\text{top, bottom, left cap, right cap}\}$ , compute the collision time  $t_{n,w}$  analytically:

- Flat walls:  $t = (y_{\text{wall}} - y)/v_y$  if approaching
- Circular caps: solve quadratic  $|\mathbf{r} + \mathbf{v}t - \mathbf{c}|^2 = R^2$  for smallest positive  $t$

### Main loop:

1. Find the minimum collision time  $t^* = \min_{n,w} t_{n,w}$
2. If  $t^* > T_{\text{end}}$ , advance all particles to  $T_{\text{end}}$  and terminate
3. Advance all particles:  $\mathbf{r}_n \rightarrow \mathbf{r}_n + \mathbf{v}_n(t^* - t_{\text{current}})$
4. Reflect the colliding particle's velocity off the wall normal
5. Update collision times for the affected particle only
6. Repeat

This algorithm has complexity  $O(N_{\text{collisions}} \cdot M)$  per time evolution, where  $N_{\text{collisions}} \sim M \cdot T/\tau_{\text{coll}}$  and  $\tau_{\text{coll}} \sim 1$  is the mean collision time.

### 10.3 Parameters

| Parameter        | Value   |
|------------------|---|
| Stadium geometry | $R = 1, a = 1$                                  |
| Particle speed   | $ v  = 1$                                       |
| Perturbation     | $\varepsilon = 0.01$                            |
| Time range       | $T \in [1, 25]$ (25 values)                     |
| Ensemble sizes   | $M \in [49, 4999]$ (30 log-spaced values)       |
| Coarse-graining  | $\delta \in [0.02, 2.0]$ (30 log-spaced values) |
| Random seed      | 42 (reproducibility)                            |

The parameter ranges were chosen as follows. The perturbation  $\varepsilon = 0.01$  is small enough that linearized dynamics applies near the reversal point, but large enough to produce measurable effects within the simulation window. The coarse-graining range  $\delta \in [0.02, 2]$  spans from just above  $\varepsilon$  (where immediate failure occurs) to the system size (where all trajectories “return”). The time range  $T_{\text{max}} = 25$  corresponds to approximately 25 Lyapunov times.

### 10.4 Results

**Sigmoid decay.** Fidelity curves (Main Text Fig. 3f) exhibit the characteristic sigmoid shape predicted by the geometric mechanism. The transition from  $F \approx 1$  to  $F \approx 0$  occurs over a narrow time window, consistent with threshold crossing rather than exponential leakage.

**Critical time scaling.** The critical time  $t_c$ —defined as the time where  $F = 0.5$ —scales linearly with  $\ln(\delta/\varepsilon)$  as predicted:

$$t_c = \frac{1}{\lambda} \ln \left( \frac{\delta}{\varepsilon} \right) \quad (19)$$

Linear regression yields slope  $1/\lambda = 3.49 \pm 0.05$ , corresponding to  $\lambda \approx 0.29$ . This is consistent with literature values for the stadium Lyapunov exponent.

**$M$ -independence.** The critical time shows negligible dependence on ensemble size, with mean relative variation  $\sigma_{t_c}/t_c < 2.5\%$  across  $M \in [49, 4999]$ . This confirms that irreversibility emerges from individual trajectory geometry rather than statistical effects. The near-horizontal contours in Main Text Fig. 3b provide visual confirmation.

## 10.5 Saturation Artifact

At large  $\delta$  (small  $\ln(\delta/\varepsilon)$ ), the fitted  $t_c$  exceeds the simulation window  $T_{\max} = 25$ . These points represent cases where fidelity never drops below 0.5 within our simulation time—not because reversal succeeds, but because our coarse-graining is so coarse that most trajectories appear to “return” regardless of dynamics.

Physically, when  $\delta$  approaches the system size ( $\sim 2$  in natural units), the criterion for “return” becomes trivially satisfied. These saturated points (gray in Main Text Fig. 3c) are excluded from the linear fit. The saturation threshold  $t_c > 0.8 T_{\max} = 20$  cleanly separates the physical scaling regime from the finite-time artifact.

## 10.6 Code Availability

Python simulation code is available at [<https://github.com/beastraban/Stadium-Billiard-Loschmidt-Echo>]. The collision table implementation follows the event-driven molecular dynamics approach of Haile (1992), adapted for billiard geometry.

# 11 Speculative Extension: Planck-Scale Horizons (Non-Essential)

**Note:** This section presents a speculative extension of the geometric framework. It is not required for the resolution of Loschmidt’s paradox, which stands independently on the arguments in the main text and preceding supplementary sections.

## 11.1 Motivation

The geometric mechanism operates wherever chaos meets a resolution threshold. We have demonstrated this at the scale of molecular dynamics ( $\hbar$ ) and numerical simulation ( $\varepsilon$ ). A natural question is whether the same principle might extend to the Planck scale—though this remains conjecture.

## 11.2 The Bekenstein-Hawking Puzzle

The Bekenstein-Hawking entropy [1, 2]:

$$S_{BH} = k_B \frac{A}{4\ell_p^2} \quad (20)$$

assigns each Planck cell only  $\ln d = 1/4$  nats—an effective alphabet size  $d = e^{1/4} \approx 1.284$ , far less than one bit. While various frameworks have derived this coefficient—string theory microstate counting [3], loop quantum gravity spin networks [4], Euclidean path integrals [5]—its geometric meaning remains unclear.

### 11.3 A Possible Geometric Interpretation

If horizon dynamics involve Lyapunov instability, as suggested by the holographic scrambling bound [6], stable manifolds would contract into fractal structures at the Planck scale. The Kaplan-Yorke formula [7] relates Hausdorff dimension to Lyapunov exponents. A fractal with  $D_H = e^{1/4} \approx 1.284$ —intermediate between curve ( $D = 1$ ) and surface ( $D = 2$ )—would partially fill each Planck cell (Fig. 1), encoding exactly:

$$S_{BH} = k_B \frac{A}{\ell_p^2} \times \ln(D_H) = k_B \frac{A}{4\ell_p^2} \quad (21)$$

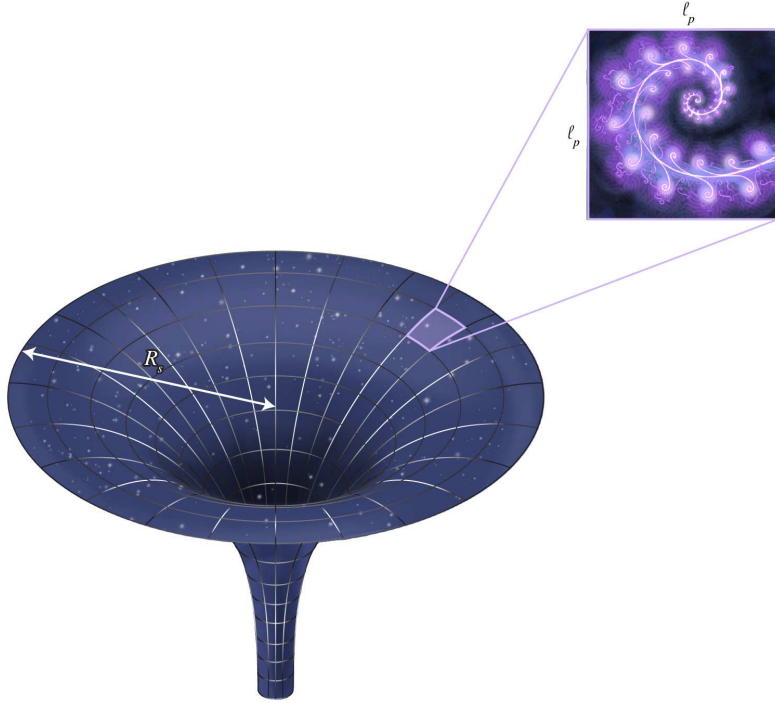


Figure 1: **Conjectured fractal information encoding at the Planck scale.** If the geometric mechanism extends to horizons, each Planck cell would contain fractal sub-structure with Hausdorff dimension  $D_H = e^{1/4} \approx 1.284$ , encoding  $\ln(D_H) = 1/4$  nats per cell.

### 11.4 Significant Caveats

This interpretation is highly speculative and faces significant challenges:

- The connection between horizon dynamics and classical Lyapunov instability remains unclear
- The Kaplan-Yorke formula applies to dissipative systems; its extension to Hamiltonian or quantum-gravitational contexts is non-trivial
- The numerical coincidence  $\ln(D_H) = 1/4$  may not reflect deeper physics
- We have no independent calculation of the horizon's effective Lyapunov spectrum

## 11.5 Why Include This Speculation?

If correct, this interpretation would suggest a single geometric mechanism—chaotic dynamics meeting quantum resolution—operating from molecular collisions to black hole horizons. The factor of 1/4 would then encode fractal dimension rather than appearing as unexplained numerology.

We present this possibility not as a claim but as a direction for future investigation. The resolution of Loschmidt’s paradox in the main text does not depend on this extension in any way.

## References

- [1] Bekenstein, J. D. Black holes and entropy. *Phys. Rev. D* **7**, 2333–2346 (1973).
- [2] Hawking, S. W. Particle creation by black holes. *Commun. Math. Phys.* **43**, 199–220 (1975).
- [3] Strominger, A. & Vafa, C. Microscopic origin of the Bekenstein-Hawking entropy. *Phys. Lett. B* **379**, 99–104 (1996).
- [4] Ashtekar, A., Baez, J., Corichi, A. & Krasnov, K. Quantum geometry and black hole entropy. *Phys. Rev. Lett.* **80**, 904–907 (1998).
- [5] Gibbons, G. W. & Hawking, S. W. Action integrals and partition functions in quantum gravity. *Phys. Rev. D* **15**, 2752–2756 (1977).
- [6] Maldacena, J., Shenker, S. H. & Stanford, D. A bound on chaos. *J. High Energy Phys.* **2016**, 106 (2016).
- [7] Kaplan, J. L. & Yorke, J. A. in *Functional Differential Equations and Approximations of Fixed Points* 204–227 (Springer, 1979).